

Hydrodynamic Performance of the Ship Propeller under Oscillating Flow with and Without Stator

Alireza Nadery*, Hassan Ghassemi

Department of Maritime Engineering, Amirkabir University of Technology, Tehran, Iran

*Corresponding author: alireza.nadery33@gmail.com

Received April 03, 2020; Revised May 05, 2020; Accepted May 12, 2020

Abstract This paper is numerically presented the effect of the pre-swirl stator (or say stator) on the hydrodynamic performance of the ship propeller. The flow is oscillating into the propeller that is the same at each radius. The propeller is selected KP505 and the stator is 4 blades mounted at upstream of the propeller. With a computational fluid dynamics (CFD) method based on the general CFD by STAR-CCM+ Solver, the thrust and torque coefficients for one blade and whole blades during one cycle, the pressure at a specific on the back and face sides of the propeller and axial and cross velocities are presented and discussed.

Keywords: ship propeller, stator, pressure distribution, thrust and torque coefficients

Cite This Article: Alireza Nadery, and Hassan Ghassemi, "Hydrodynamic Performance of the Ship Propeller under Oscillating Flow with and Without Stator." *American Journal of Civil Engineering and Architecture*, vol. 8, no. 2 (2020): 56-61. doi: 10.12691/ajcea-8-2-5.

1. Introduction

One of proper and simple energy saving device (ESD) is to use stator for improving the propeller efficiency. It is installed in front of the propeller behind the ship hull. This paper focuses on the stator device providing the possibility to reduce the rotational losses incurred by the propeller [1]. Also, this device modifies the loading of the propeller blades, through which the delivered thrust per unit of torque is raised.

Stator is a one good and simple type of the ESD as a possible solution to enhance the efficiency. The number of blades of the PSS is usually 3 to 5, which are mounted upstream of the propeller. The task of the PSS is to modify the axial and tangential velocity components of the inflow on the propeller. During last two-decades, various PSS are designed and mounted for energy saving of the ship. For example, Daewoo have launched the newest solution in its propulsive efficiency. The new Daewoo device is an energy saving solution designed to reduce the power losses that occur in a ship's propeller's slipstream, improving fuel efficiency by up to 6% with additional reduction in cavitation. Figure 1 shows the stator designed by Daewoo.

Regarding to energy saving, there are many approaches on the ship hull to reduce drag and on the propulsor to increase the efficiency [2,3,4]. Sharifi et al presented various innovative technologic devices in shipping energy saving and diminish fuel consumption [5]. Focusing to the stator effect to the propeller, there are some published papers regarding to this subject. Çelik and Güner [6] studied pre-swirl stator (PSS) using lifting line theory and CFD. Shin et al [7] studied two kinds of pre-swirl

duct (PSD) i.e., unconventional half circular duct and conventional circular pre-swirl duct for VLCC ship with large block coefficients using experiment and CFD. A new technique for developing the results from the model to the full scale of a ship equipped with PSSs is suggested by [8]. In 2015, Kim studied a new PSD for 317 KVLCC and indicated that using this PSD results in improving the propulsive efficiency by recovering the wake fraction [9]. The vortex-lattice method and CFD-based approach is used by [10] to investigate the hydrodynamic design of a PSS in various operating conditions. Hanaoka et al [11] predicted the open-water thrust and torque of propellers equipped with PSD at different distance of the propeller and duct using the quasi-continuous method and indicated that different distance of duct in front of the propeller has insignificant impact on open-water characteristics of the propeller.



Figure 1. Daewoo stator mounted to the ship

A lifting surface model is used for determining both propeller and stator blade's pitch and camber in direct way and compared with viscous fluid model-based RANSE

approach by [12]. Three types of PSD using CFD and experiment are compared and shown Mewis duct provided the highest value of thrust and torque coefficients at higher advance ratios [13].

The rest of this paper is structured as follows. In Section 2, governing equations are described. Numerical results of the hydrodynamic coefficients of the model propeller and effect of the stator are presented in Section 3. Finally, conclusion is presented in Section 4.

2. Governing Equations

In 3D CFD simulation, Navier-Stokes equations and continuity equation are governed. These equations can be written in a Cartesian tensor form as:

$$\frac{\partial u_i}{\partial x_i} = 0 \quad (1)$$

$$\begin{aligned} \frac{\partial}{\partial t}(\rho u_i) + \frac{\partial}{\partial x_i}(\rho u_i u_j) = -\frac{\partial p}{\partial x_i} \\ + \frac{\partial}{\partial x_j} \left[\mu \left(\frac{\partial u_i}{\partial x_j} + \frac{\partial u_j}{\partial x_i} \right) \right] + \frac{\partial}{\partial x_j} (-\rho \overline{u_i' u_j'}) \end{aligned} \quad (2)$$

where x_i are Cartesian coordinates, u_i are the corresponding velocity components and p , ρ and μ are the pressure, density, and viscosity, respectively. Moreover, the steady-state solution of governing Eqs. (1) and (2) are also considered (i.e. $\partial(\rho u_i)/\partial t = 0$). In the present study, STAR-CCM+ commercial software is used which discretizes the continuous equations using the finite volume method. Grid independence is the addition of the number of an element to obtain a constant value, so that the numerical result close to the experiment result. We tried with different mesh numbers for the propeller alone and propeller with stator. According to our experience, it was discovered that by using 2 million meshes for propeller and 2.5 million meshes for the propeller and stator are found to be the appropriate choice as the final mesh based on the acceptable error and the simulation time.

In order to resolve accurately the boundary layer and provide desired levels of wall y^+ , three layers of prismatic cells are placed. The total thickness of the prism layer is about 1.6% of the propeller radius. With such settings of the boundary layer mesh achieves the y^+ values less than 40. The selected time step has been calculated in such a way that the propeller rotates between 0.5 and 2° per time step according to International Towing Tank Conference (ITTC) recommendation [14]. The $k-\varepsilon$ turbulence model was used to close the Reynolds stress term of $-\rho \overline{u_i' u_j'}$ and the moving reference frame (MRF) scheme was adopted for the rotation of the propeller in some calculation. Further details of the implementation can be found in the STAR-CCM+ manuals and [15].

The results from the simulation with regard to the thrust coefficient (K_T), torque coefficient (K_Q), open water efficiency (η_o) and advance coefficient (J) are expressed as follows:

$$\begin{aligned} K_T = \frac{T}{\rho n^2 D^4}, \quad K_Q = \frac{Q}{\rho n^2 D^5} \\ \eta_o = \frac{J K_T}{2\pi K_Q}, \quad J = \frac{V_a}{nD} \end{aligned} \quad (3)$$

where ρ is the density of water, n is revolutions per second of the propeller, D is the diameter and V_a is the velocity of advance.

3. Numerical Results

3.1. Propeller Type

The propeller is rotating speed n and the uniform flow is entered to the propeller with advance speed V_a , which is called propeller open water condition. The propeller is selected a model propeller KP505, which designed and tested by the Korean research institute of ship and ocean engineering (KRISO) for KRISO container ship called KCS. The main dimensions are given in Table 1. These numerical models applied in this study were implemented using STAR-CCM+. The propeller is rotated with 10.60 rps and advance speed is changed to get advance coefficient from $J=0.15$ to $J=0.95$ by step 0.1. So, the results of thrust, torque and efficiency are calculated at nine advance coefficients. Comparison of the hydrodynamic coefficients of this model propeller were calculated and presented by authors [16].

Table 1. Main dimensions of the KP505

Parameter	Dimension
Diameter (D)	250 [mm]
No. of blades	5
Pitch ratio (mean)	0.950
Hub ratio	0.180
Expanded area ratio	0.80
Section type	NACA66
Rotation	RH

3.2. Oscillating Velocities

The thrust and torque of a propeller operating behind a ship are not constant even when the ship is moving at a constant speed in calm water with the propeller running at a fixed rpm. Fluctuations in the thrust and torque arise because the flow into the propeller varies along the circumference at each radius. This results in a periodic variation of the relative velocity of the flow with respect to a point on the propeller, and produces an unsteady loading on the propeller blades.

In this paper, the axial and tangential components of the inflow wake velocity into the propeller disc typically vary around the circumference at a given radius r . Let's define $V_a(\theta)$ and $V_t(\theta)$ are the axial and tangential velocities, respectively, and θ the angle measured from the vertical upward. It can be represented the non-uniform wake velocity field including tangential and axial components via the Fourier series as follows:

$$V_a(r, \theta) = \sum_{m=0}^{10} a(r) \cos(m\theta) + a'(r) \cos(m\theta), \quad (4)$$

$$V_t(r, \theta) = \sum_{m=0}^{10} b(r) \cos(m\theta) + b'(r) \cos(m\theta)$$

where a , b , a' and b' are Fourier coefficients. In practice, only a limited set of harmonic components are used. In this paper $m=10$ is considered for both computations.

Figure 2 shows the axial and tangential velocities in one circle at $r=0.7R$. And also, the contour and vector wake velocity distribution at propeller plane are presented in Figure 3. The radial velocity is neglected for very small value relative to other two velocities.

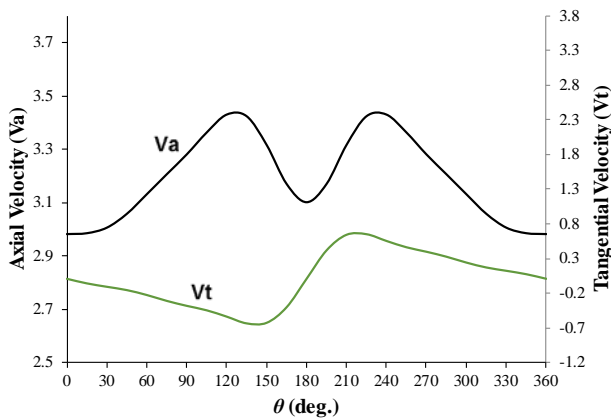


Figure 2. Axial (V_a) and tangential (V_t) velocities in one circle at $r=0.7R$

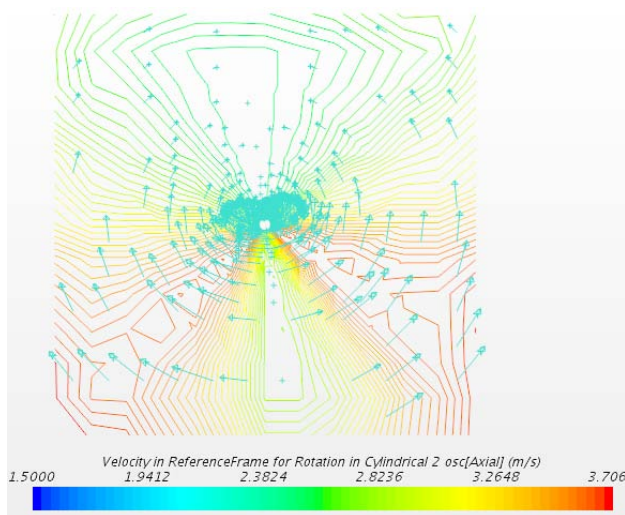


Figure 3. Axial (isolines) and cross velocities (vector) distribution.

3.3. Stator Effect

The main role of stator is to reduce the slip loss of the propeller encountered in rotation. The stator rotates flow in opposite direction of propeller rotation and increases thrust and torque. The design of stator is important to generate the proper flow direction to the propeller; otherwise it causes to add resistance. In this study, stator is to be designed by 4 blades, span-chord ratio is 0.15, NACA0006 section and its angle of attack ± 10 , means right and left sides are opposite angles to compensate the propeller rotation. Its distance to the propeller is 0.17D.

Main dimensions of the stator are given in Table 2. Surface solid mesh of the propeller and stator is shown in Figure 4.

Here, our calculations are based on the thrust identity, which means total thrust ($T_{total} = T_{prop} - T_{stator}$, where T_{stator} is the drag of stators) and advance speed (V_a) are the same in the case of propeller with and without stator. In order to adapt this condition, the propeller rotation speed is changed to reach the same total thrust. That means with and without stator, the speed and total thrust are 3.1711 m/s and 80 N, respectively, while the rotating speeds (n) are different, causes to change torque, delivered power and efficiency. In case of with stator, it is difficult to find n to reach the same thrust. The rotating speed of the propeller (n) is calculated by trial and error and takes consuming time. The calculation results are given in Table 3. As can be seen, the delivered power is diminished about 2.3% and efficiency is increased with stator.

Table 2. Main dimensions of the stator

Parameter	Value
Section type	NACA-0006
Chord	0.15D
Span	1D
No. of stators	4
Angle of attack [deg.]	± 10
Distance to propeller	0.17D

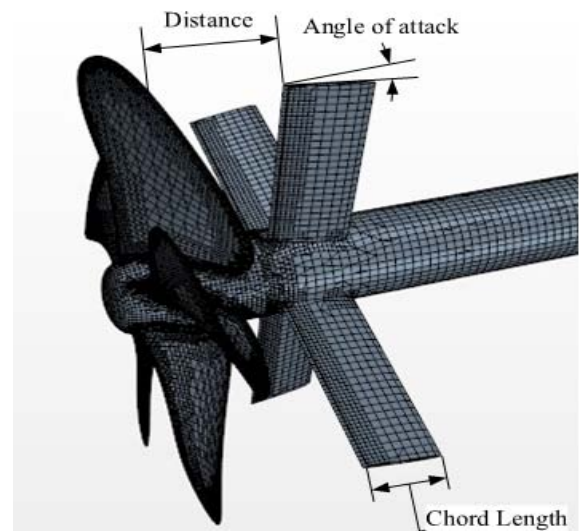


Figure 4. Surface mesh of the propeller and stator

Table 3. Performance of the propeller with and without stator under oscillating and cross-flow

Parameter	unit	w/o stator	with stator
V_a (mean)	[m/s]	3.1711	3.1711
n	[rps]	15.307	14.547
J	[-]	0.8286	0.8719
K_T	[-]	0.0883	0.0963
T_{total}	[N]	80.793	79.579
$10K_Q$	[-]	0.2003	0.2283
Q	[N-m]	4.5760	4.7092
η	[-]	0.5814	0.5849
$P_d = 2\pi n Q$	[W]	440.39	430.75

Thrust and torque coefficients against one cycle for one blade and whole blades with and without stator at 0.82 advance coefficient are shown in Figure 5. There are some fluctuation loading for one blade (left) during one cycle. The effect of stator makes some fluctuations on the thrust and torque coefficients while without stator the results are constant during one cycle or revolution. However, the mean total thrust and torque coefficients are increased during one cycle.

Figure 6 shows the pressure distribution contours at back and face sides of the propeller with and without stator at $J=0.82$. As shown, it is evident that high pressure

is found at face or pressure side and low pressure is shown in back or suction side. The stator has reduced the maximum absolute value of the pressure on the suction side, which is useful for preventing the cavitation. Figure 7 also shows that the pressure fluctuations are reduced in the four rotation cycles in back and face side.

Axial (isolines) and cross velocities (vector) with stator (right) and without stator (left) are presented at advance coefficient of 0.82 at $x=0.2D$, as shown in Figure 8. As can be observed, stator causes to change the flow into the propeller, especial the cross velocities directions.

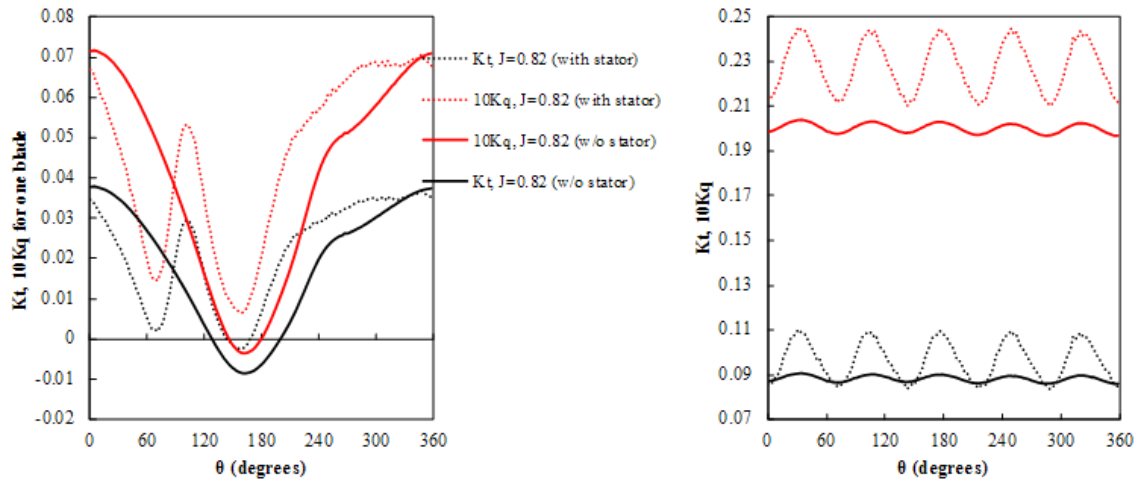


Figure 5. Thrust and torque coefficients in one cycle for one (left) and whole blades (right) with and without stator under oscillating and cross-flows

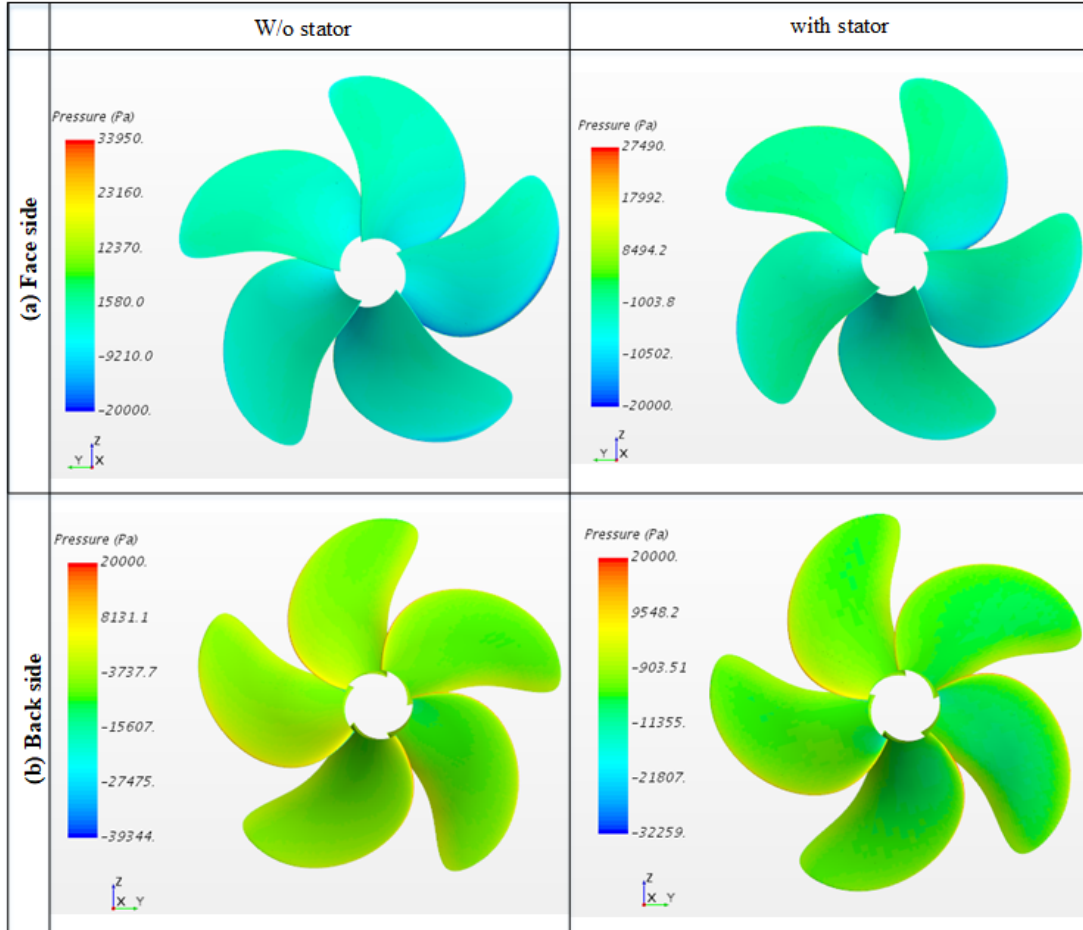


Figure 6. Pressure distribution contours on propeller surfaces at $J=0.82$ under oscillating and cross-flow

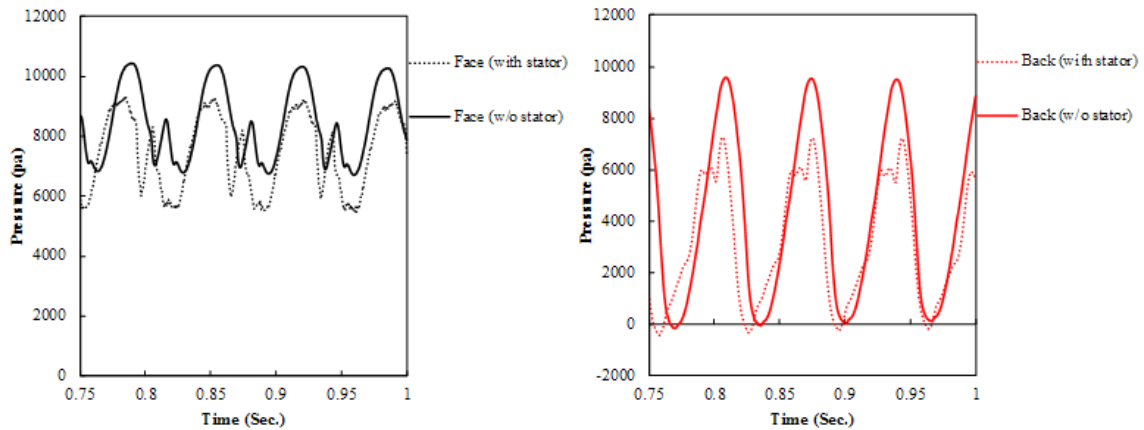


Figure 7. Fluctuating pressure for four cycles for face (left) and back side (right) at $r/R=0.7$ and $x/C=0.4$ under oscillating and cross-flows, $Va=3.1711$

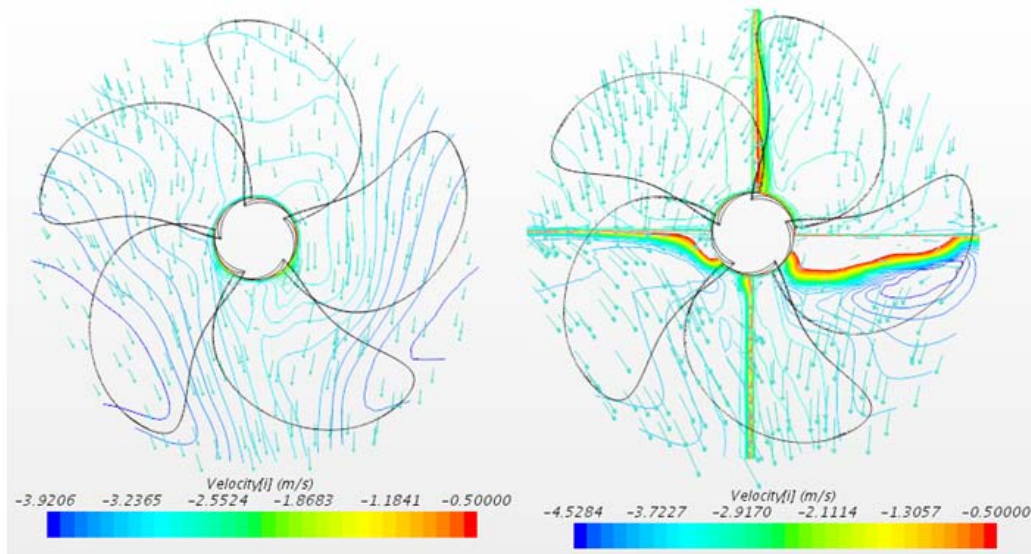


Figure 8. Axial (isolines) and cross velocities (vector) with stator (right) and without stator (left) ($x/D=0.2$ and $J=0.82$) under oscillating and cross-flows

4. Conclusions

This study was numerically investigated the hydrodynamic performance of the propeller in oscillating flows with and without stator. The results of the present study lead to the following conclusions:

- The thrust and torque coefficients are affected by the stator that is given bigger amplitude.
- Delivered power with stator was saved about 2.3%.
- Flow filed was affected by the stator, especially tangential velocity into the propeller.

References

- [1] Lee, J. T., Kim, M. C., Suh, J. C., Kim, S. H., and Choi, J. K., (1992), "Development of a Preswirl statorpropeller system for improvement of propulsion efficiency: A Symmetric Stator Propulsion System," *Transaction of SNAK*, 29.
- [2] Heidarian, A., Ghassemi, H., and Liu, P., (2018), "Drag reduction by using the microriblet of sawtooth and scalloped types," *International Journal of Physics*, 6(3), pp. 93-98.
- [3] Javadpour, S. M., Eskafi Noghani, A., Ghassemi, H., and Molyneux, D., (2019), "Hydrodynamic Characteristics of the propeller-rudder interaction by RANS solver," *American Journal of Mechanical Engineering*, 7(1), pp. 35-40.
- [4] Maghareh, M., and Ghassemi, H., (2017), "Propeller efficiency enhancement by the blade's tip reformation," *American Journal of Mechanical Engineering*, 5(3), pp. 70-75.
- [5] Sharifi, Y., Ghassemi, H., and Zanganeh, H., (2017), "Various innovative technologic devices in shipping energy saving and diminish fuel consumption," *International Journal of Physics*, 5(1), pp. 21-29.
- [6] Çelik, F., and Güner, M., (2007), "Energy Saving device of stator for marine propellers," *Ocean Engineering*, 34(5-6), pp. 850-855.
- [7] Shin, H. J., Lee, J. S., Lee, K. H., Han, M. R., Hur, E. B., and Shin, S. C., (2013), "Numerical and experimental investigation of conventional and un-conventional preswirl duct for VLCC," *International Journal of Naval Architecture and Ocean Engineering*, 5(3), pp. 414-430.
- [8] Park, S., Oh, G., Hyung Rhee, S., Koo, B. Y., and Lee, H., (2015), "Full scale wake prediction of an energy saving device by using computational fluid dynamics," *Ocean Engineering*, 101, pp. 254-263.
- [9] Kim, J. H., Choi, J. E., Choi, B. J., Chung, S. H., and Seo, H. W., (2015), "Development of Energy-saving devices for a full slow-speed ship through improving propulsion performance," *International Journal of Naval Architecture and Ocean Engineering*, 7(2), pp. 390-398.
- [10] Saettone, S., Regener, P. B., and Andersen, P., (2016), "Pre-Swirl Stator and Propeller Design for Varying Operating Conditions," *Proceedings of the 13th International Symposium on PRACTical Design of Ships and Other Floating Structures*.
- [11] Hanaoka, A., Kawanami, Y., and Hinatsu, M., (2016), "Application of quasi-continuous method to open-water characteristics

- predictions of propellers with energy-saving ducts,” *International Journal of Offshore and Polar Engineering*, 26, pp. 72-80.
- [12] Król, P., Bugalski, T., and Wawrzusiszyn, M., (2017), “Development of numerical methods for marine propeller - pre-swirl stator system design and analysis,” *Proceedings of the Fifth International Symposium on Marine Propulsors*, Espoo, Finland.
- [13] Nowruzi, H., and Najafi, A., (2019), “An experimental and CFD study on the effects of different pre-swirl ducts on propulsion performance of series 60 ship,” *Ocean Engineering*, 173(424), pp. 491-509.
- [14] ITTC Proceedings, (2014), “Practical Guidelines for Ship CFD Applications ITTC - Recommended Procedures and Guidelines, Section 7.5-03-02-03,” *International Towing Tank Conference*.
- [15] Chamanara, M., and Ghassemi, H., (2016), “Hydrodynamic characteristics of the Kort-nozzle propeller by different turbulence models,” *American Journal of Mechanical Engineering*, 4(5), pp. 169-172.
- [16] Nadery, A., and Ghassemi, H., (2020), “Toward the hydrodynamic performance of the propeller behind the ship by pre-swirl stator,” *Journal of Engineering for the Maritime Environment*. under review.



© The Author(s) 2020. This article is an open access article distributed under the terms and conditions of the Creative Commons Attribution (CC BY) license (<http://creativecommons.org/licenses/by/4.0/>).